Dielectric Relaxation of *cis*-Polyisoprene Chains in Oligo- and Polybutadiene Matrices: Matrix Effects on Mode Distribution and Relaxation Time

Hiroshi Watanabe,*,† Osamu Urakawa,‡ Hirofumi Yamada,§ and Ming-Long Yao⊥

Institute for Chemical Research, Kyoto University, Uji, Kyoto 611, Japan, Department of Macromolecular Science, Faculty of Science, Osaka University, Toyonaka, Osaka 560, Japan, and Rheometric Scientific F.E. Ltd., 2-19-6 Yanagibashi, Taito-ku, Tokyo 111, Japan

Received June 1, 1995; Revised Manuscript Received October 12, 1995[⊗]

ABSTRACT: The dielectric behavior of dilute *cis*-polyisoprenes (PI) chains was examined in matrices of oligo- and polybutadiene (B) chains of various molecular weights M_B. The PI chains had type-A dipoles parallel along their contour so that their global motion was dielectrically detected. Specifically, the matrix effects were examined for the dielectric mode distribution as well as for the longest and second longest relaxation times, $\tau_{1,\epsilon}$ and $\tau_{2,\epsilon}$. $\tau_{1,\epsilon}$ and $\tau_{2,\epsilon}$ were determined from dielectric loss (ϵ'') peak frequencies for PI chains without and with (symmetrical) inversion of the type-A dipoles. These relaxation times were compared at an isofrictional state: For this purpose, the relaxation times for the PI chains in short matrices of M_B < 9K (having excess free volume) were corrected with factors ζ^∞/ζ, with ζ being the segmental friction for PI in those matrices and ζ^∞ being the ζ value in long matrices of M_B > 9K. As done by Colby et al. (*Macromolecules* **1987**, *20*, 2226), those ζ-correction factors were determined from standard WLF analysis for the time−temperature shift factor a_T. For long PI chains ($M_I \cong 48$K) with and without dipole inversion, the relaxation times hardly depended on M_B in the nonentangling matrices but increased with M_B in entangling matrices (in a constraint release regime). On the other hand, $\tau_{1,\epsilon}$ of a short PI chain ($M_I \cong 6$K) was found to be independent of M_B in both entangling and nonentangling matrices. More importantly, for both long and short PI chains, the dielectric mode distribution was found to be broadened with increasing M_B. This change in the mode distribution was not due to changes in the entanglement effects, the excluded volume interaction, and the hydrodynamic interaction. Instead, coupling of the motion of the PI and matrix chains appeared to have led to the mode broadening. The broadening was completed in a rather narrow crossover zone of M_I and M_B: In that zone, a ratio of $\tau_{1,\epsilon}$ to the longest (viscoelastic) relaxation time of the matrix, $\tau_{1,G}$, was not constant but strongly dependent on $\tau_{1,G}$. This fact indicated that the coupling of PI and matrices was not of simple viscoelastic nature, for which the $\tau_{1,\epsilon}/\tau_{1,G}$ ratio should be essentially constant in the crossover zone.

I. Introduction

cis-Polyisoprene (PI) chains have so-called type-A dipoles[1,2] parallel along the chain contour so that their global motion induces molecular weight (M_I)-dependent dielectric relaxation. This unique feature enables us to dielectrically investigate polymer dynamics at long time scales, and extensive studies have been made for PI in bulk,[3−5,7−9,14] blends,[6,8,10,11,15] and solutions.[4,8,12,13,16,17] Most of the studies were carried out for *regular* PI chains having dipoles parallel in the *same direction* along the chain contour.[3−6,8,9,11−13,16]

For those chains, end-to-end vector fluctuation is dielectrically detected, and corresponding dielectric loss (ϵ'') is decomposed into modes,

$$\epsilon''(\omega) = \sum_p g_p \frac{\omega\tau_{p,\epsilon}}{1 + \omega^2\tau_{p,\epsilon}^{\ 2}} \qquad (1)$$

Here, g_p and $\tau_{p,\epsilon}$ are the intensity and relaxation time for the pth dielectric mode. As noted from eq 1, the behavior of the PI chains is characterized with the longest relaxation time $\tau_{1,\epsilon}$ and the mode distribution: The mode distribution is determined by the relaxation time span ($\tau_{p,\epsilon}/\tau_{1,\epsilon}$ ratio) and the intensity distribution (g_p/g_1 ratio).

For $\tau_{1,\epsilon}$ of the regular PI chains, results of the studies so far carried out are summarized as follows. In monodisperse bulk states, $\tau_{1,\epsilon}$ at an isofrictional state is proportional to $M_I^{3.5}$ and M_I^2 in the entangled and nonentangled regimes, respectively.[3−5,7,8] For dilute probe PI chains in homogeneous blends with entangling matrices of molecular weight M_{mat}, the M_I and M_{mat} dependencies of $\tau_{1,\epsilon}$ become weaker and stronger, respectively, with decreasing M_{mat}.[6,10,11] These changes in the M dependence are attributed to changes in the entanglement lifetime[10,11] (due to constraint release[18−20] by the matrix motion). Finally, in solutions in low molecular weight solvents, the M_I dependence of $\tau_{1,\epsilon}$ becomes weaker with decreasing PI concentration c_I and approaches the dependence expected for bead−spring models.[12,13,17] All these results are in harmony with the well-known behavior of the longest *viscoelastic* relaxation time.[21]

On the other hand, a very prominent difference exists between dielectric and viscoelastic relaxation mode distribution: The dielectric mode distribution of regular PI chains is quite insensitive to the existence of entanglement (in the monodisperse state) and to changes in the entanglement lifetime (in the blends),[10,11,15] while

* To whom correspondence should be addressed.
† Kyoto University (previously at Osaka University).
‡ Osaka University (current address: Department of Polymer Science and Engineering, Kyoto Institute of Technology, Matsugasaki, Sakyo-ku, Kyoto 606, Japan).
§ Osaka University (current address: Department of Materials Science, Japan Advanced Institute of Science and Technology, Hokuriku, Nomi, Ishikawa 923-12, Japan).
⊥ Rheometric Scientific F.E. Ltd.
⊗ Abstract published in *Advance ACS Abstracts,* December 15, 1995.

0024-9297/96/2229-0755$12.00/0

the viscoelastic mode distribution drastically changes with these factors.[21] This difference results from the different nature of the dielectric and viscoelastic relaxation, the former reflecting orientational correlation of chain bond vectors at two separate times and the latter detecting anisotropy of bond orientation at respective times.[11,14,15,17]

Nevertheless, changes have been found also for the dielectric mode distribution:[12,13,16,17] In dilute solutions of regular PI chains, the mode distribution is sharp and close to that for bead−spring models. However, with increasing c_I above the overlapping concentration c^*, the mode distribution becomes broader. Finally, at $c_I \geq 8c^*$ the distribution coincides with that for bulk PI. Despite these clear changes in the dielectric behavior, the data for regular PI are not sufficient for specifying whether the mode broadening is due to changes in the $\tau_{p,\epsilon}$ span or the g_p distribution (cf. eq 1).

An answer for this problem is found from dielectric studies for a special sort of PI chains having *once-inverted* dipoles.[7,10,14,15,17] For these dipole-inverted chains as well as regular PI chains (without inversion), fundamental dielectric features are described by a local correlation function,[10,11,14,15,17]

$$C(n,t;m) = (1/a^2)\langle \mathbf{u}(n,t)\cdot\mathbf{u}(m,0)\rangle \qquad (2)$$

Here, $\mathbf{u}(n,t)$ is a bond vector for the nth segment at time t and $a^2 = \langle \mathbf{u}^2\rangle$. This function represents orientational correlation of bond vectors at two separate times and is decomposed into its eigenmodes at long time scales of global relaxation,[14,15]

$$C(n,t;m) = \frac{2}{N}\sum_{p=1}^{N} f_p(n)\, f_p(m)\, \exp(-t/\tau_p) \qquad (3)$$

Here, f_p and τ_p are the eigenfunction and relaxation time for the pth eigenmode, and N is the number of segments of the chain. For the PI chain having the dipole inversion at the n^*th segment, ϵ'' is described by eq 1 with the dielectric $\tau_{p,\epsilon}$ being given by τ_p for the pth eigenmode and g_p being determined by f_p as[14,15]

$$g_p(n^*) = 2\Delta\epsilon\left[\frac{1}{N}\int_0^{n^*} f_p(n)\, dn - \frac{1}{N}\int_{n^*}^{N} f_p(n)\, dn\right]^2 \qquad (\Delta\epsilon = \text{total intensity}) \quad (4)$$

(g_p for regular PI chains is also given by eq 4 as a special case of $n^* = 0$ or N.) Because of the n^* dependence of g_p (eq 4), ϵ'' data are remarkably different for a series of dipole-inverted PI chains having identical M_I but different n^*. This difference enables us to experimentally evaluate τ_p and $f_p(n)$ that *separately* determine $\tau_{p,\epsilon}$ and $g_p(n^*)$ and thus govern the dielectric mode distribution (cf. eq 1).

Experiments have been carried out for such a series of dipole-inverted PI chains in various environments: the monodisperse bulk state,[14] blends with entangling polybutadiene matrix of $M = 9.24$K,[15] and solutions in oligobutadiene of $M = 0.7$K.[17] Those experiments revealed that the τ_p span is nearly the same in the three environments but f_p is quite different: In the blends and bulk state, $f_p(n)$ exhibits nearly the same, nonsinusoidal n dependence.[14,15] On the other hand, in the solutions, nearly sinusoidal $f_p(n)$ at $c_I \leq c^*$ becomes distorted and nonsinusoidal with increasing $c_I > c^*$, and $f_p(n)$ at $c_I \geq 8c^*$ coincides with $f_p(n)$ for bulk PI.[17] These results indicate that the changes in the mode distribution observed for the PI solutions are essentially due to changes in the g_p distribution that result from changes in the n dependence of $f_p(n)$.[17]

Table 1. Characteristics of Samples

code	$10^{-3}M$	M_w/M_n
	Polyisoprenes[a]	
I-6[c]	6.12[e]	1.08
I-49[c]	48.8[e]	1.05
I-I 24-24[d]	47.7[e]	1.06
	Oligo- and Polybutadienes[b]	
B-0.7	0.711[f]	1.08
B-1	1.25[f]	1.07
B-3	2.70[f]	1.04
B-5	5.40[f]	1.02
B-6	5.95[e]	1.05
B-9	9.24[e]	1.07
B-20	19.9[e]	1.06
B-89	89.0[e]	1.05

[a] Cis:trans:vinyl ≅ 75:20:5. [b] Cis:trans:vinyl ≅ 40:50:10. [c] Without type-A dipole inversion. [d] With symmetrical type-A dipole inversion. [e] Weight-average molecular weight. [f] Number-average molecular weight.

At this point, we note that c_I is not the only factor that affects the dielectric mode distribution: In the dilute solutions and blends explained above, the dipole-inverted PI chains were equally dilute and surrounded by chemically identical matrices, oligo- and polybutadiene. Nevertheless, the mode distribution was sharp in the former but broad in the latter. From this fact, we naturally expect that the matrix (or solvent) relaxation time determined by its molecular weight is an important factor that affects the dielectric mode distribution of dilute PI chains.

For a test of this expectation, we have examined the dielectric behavior of dilute PI chains homogeneously mixed in matrices of oligo- and polybutadiene of various molecular weights ranging from 0.7K to 89K. Specifically, comparison of relaxation times for the matrix and PI chains enabled us to specify conditions that are necessary for the PI chains to exhibit narrow dielectric mode distribution. Those conditions gave a clue for discussing mechanism(s) for the mode broadening. The results are presented in this paper.

II. Experimental Section

II-1. Materials. Table 1 summarizes molecular characteristics of the PI, oligobutadiene, and polybutadiene samples, the latter two being referred to as B irrespective of their molecular weights. B-1, B-3, and B-5 samples were anionically synthesized in this study with *tert*-butyllithium in benzene, and their number-average molecular weights and heterogeneity indices M_w/M_n were determined by ^{1}H-NMR (by counting the number of B monomer units per *tert*-butyl group) and oligo-GPC. B-6 and B-89 were synthesized with *sec*-butyllithium in benzene, and I-6 in heptane, respectively. These samples were characterized by standard GPC analyses including elution volume calibration and on-line, low-angle laser light scattering. Other samples were synthesized and characterized in our previous work.[7,10,14]

Among the PI samples, I-49 and I-6 are regular PI chains without dipole inversion, while I-I 24-24 has symmetrical dipole inversion. Note that I-49 and I-I 24-24 have almost identical M_I but exhibit different dielectric behavior because of this difference in the dipole alignment.

II-2. Measurements. Homogeneous blends of the PI samples in B matrices of various M_B were prepared by first dissolving prescribed amounts of PI and B in cyclohexane and then completely removing cyclohexane. The PI content was 5% for I-49 and I-I 24-24 and 10% for I-6. Dielectric loss factors, ϵ'', were measured for those I/B blends with capacitance bridges (GR 1615A, General Radio; Precision LCR-meter 4284A, Hewlett-Packard). The time−temperature superposition was valid and the ϵ'' data were reduced at 40 °C. The

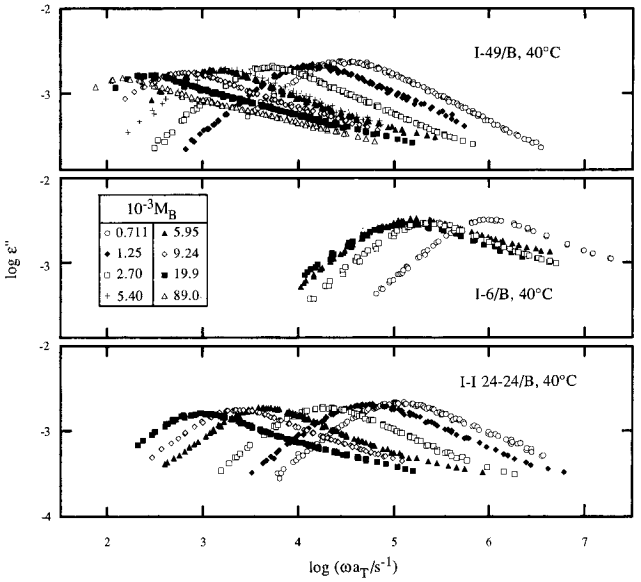

Figure 1. Frequency (ω) dependence of dielectric loss (ϵ'') at 40 °C for dilute PI chains in B matrices of various M_B as indicated. PI content: 5% (for I-49/B; top panel), 10% (for I-6/B; middle panel), 5% (for I-I 24-24/B; bottom panel). Note that I-49 and I-I 24-24 have almost identical M_I but the former has no dipole inversion while the latter has symmetrical inversion.

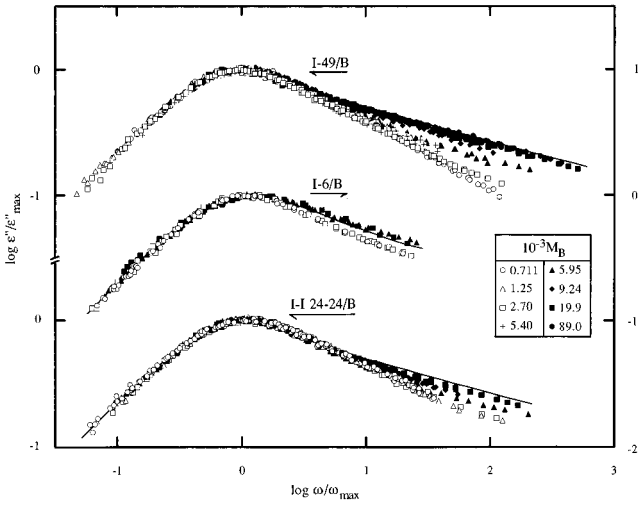

Figure 2. Comparison of shape of ϵ'' curves for the dilute PI chains examined in Figure 1. For easy comparison, the curves were reduced at their peaks. The solid curves indicate the shape of the ϵ'' curves for respective PI chains in bulk state.

shift factor a_T for ϵ'' agreed well with a_T for viscoelastic moduli of pure matrices (cf. Figure 4 shown later).

The dynamic behavior of the B matrices was characterized with viscoelastic shear moduli G^* determined with a rheometer (RDA-2, Rheometrics). The time−temperature superposition was valid and G^* data were reduced at 40 °C. From those data in the terminal (flow) zone, the zero-shear viscosity η_0 and steady-state recoverable compliance $J_e°$ were evaluated.

III. Results

III-1. Dynamic Behavior of I/B Blends and B Matrices. Figure 1 shows the frequency (ω) dependence of ϵ'' at 40 °C for the I/B blends as indicated. Data obtained in our previous study[15,17] are also shown. The B matrices had negligibly small ϵ'' at the ω examined, and the dielectric dispersions seen here are exclusively attributed to the global motion of the dilute PI chains. (Segmental motion of the PI chains is observed at much higher $\omega > 10^7$ s^{-1}.) For the I-49 and I-6 chains without dipole inversion, polarization **P** is proportional to the end-to-end vector **R** so that fluctuation of **R** is dielectrically detected. For this case, only odd eigenmodes of the local correlation function (cf. eq 3) are dielectrically observed. On the other hand, for I-I 24-24 having symmetrical dipole inversion, **P** is proportional to a difference vector $\Delta\mathbf{R} = \mathbf{R}_1 - \mathbf{R}_2$, with $\mathbf{R}_1$ and $\mathbf{R}_2$ ($=\mathbf{R} - \mathbf{R}_1$) being two end-to-center vectors. Only even modes are dielectrically active for this case.

As done in our previous paper,[17] ratios of the PI concentration c_I to the overlapping concentration c^* were evaluated from the dielectric relaxation intensities $\Delta\epsilon$ ($\propto\langle\mathbf{R}^2\rangle$) for the PI chains examined in Figure 1. The results were $c_I/c^* = 0.94-1.3$ for I-49 and I-I 24-24 ($c_I = 5\%$) in the various matrices examined and $c_I/c^* = 0.68$ for I-6 ($c_I = 10\%$). The width in the c_I/c^* values for I-49 and I-I 24-24 resulted from the excluded volume interaction that increased $\Delta\epsilon$ a little for the I-49 and I-I 24-24 chains in short matrices of $M_B \leq 2.7$K. For the shorter I-6 chain, this interaction was not significant and $\Delta\epsilon$ was constant in all B matrices examined. As judged from the c_I/c^* values, the behavior of those dilute PI chains is close to the behavior at infinite dilution.[17]

In Figure 1, we note that the ϵ'' peak for the respective PI chains shifts to the higher ω side with decreasing M_B. This shift is partly due to decrease of entanglement lifetime (constraint release)[10,11] and also to a decrease of the segmental friction ζ as explained below. We also note that the dielectric relaxation mode distribution (observed as the shape of the ϵ'' curve) becomes sharper with decreasing M_B. This change in the mode distribution is most clearly seen in Figure 2, where comparison is made for the ϵ'' curves reduced at their peaks.

As noted in Figure 2, the ϵ'' curves exhibit a sharp and almost M_B-independent shape when the matrix B chains are much shorter than the dilute PI chains. As found previously,[17] the shape of those curves is reasonably well described by bead−spring models. However, the curves become broader with increasing M_B. Finally, the shape of the curve approaches that for bulk PI (solid curves) and again becomes independent of M_B. This crossover behavior of the mode distribution is completed in a rather narrow range of M_B.

As noted also in Figure 2, the mode distribution is affected by both M_B and M_I, although effects of M_I are less significant: For the I-49 and I-I 24-24 chains in the B-6 matrix, the ϵ'' curves are sharper than the bulk curve and the mode distribution is still in the crossover regime, while for the shorter I-6 chain in the same matrix, the curve is as broad as the bulk curve. These effects of M_B and M_I on the mode distribution are discussed later in relation to the relaxation times of the PI chains and matrices.

Global motion should be almost exactly the same for the I-49 and I-I 24-24 chains having almost identical M_I (cf. Table 1). However, as explained earlier, only odd eigenmodes are dielectrically observed for the former and only even eigenmodes for the latter. Thus, we can compare the matrix effects on the odd and even modes in Figure 3, where the ϵ'' curves of I-49 and I-I 24-24 in the respective matrices are compared on a reduced frequency scale, $\omega\tau_{1,\epsilon}$ and $\omega\tau_{2,\epsilon}$. Here, $\tau_{1,\epsilon}$ and $\tau_{2,\epsilon}$ are the relaxation times for the first and second eigenmodes explained later in Figure 6. As seen in Figure 3, the ϵ'' curves of I-49 and I-I 24-24 have almost indistinguishable shape. This result indicates that the increase in M_B broadens the distribution of the odd and even modes to nearly the same extent.

In Figure 4, shift factors a_T are shown for ϵ'' of dilute PI chains in the B matrices (symbols without pips) and

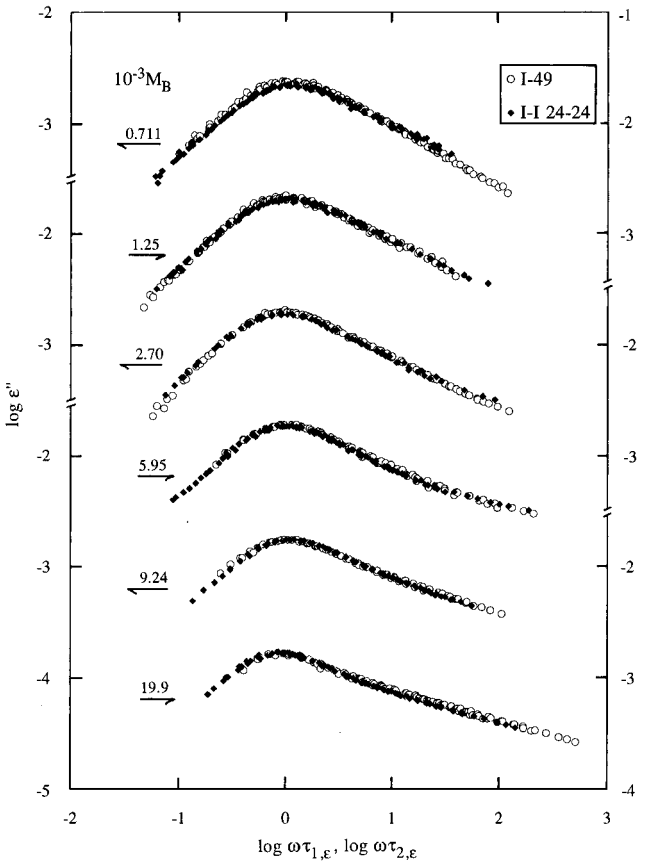

Figure 3. Comparison of ϵ'' curves for dilute I-I 24-24 and I-49 chains (5%) in various B matrices as indicated. Note that these chains have almost identical M_I but differently aligned dipoles. The curves are compared on a reduced frequency scale, $\omega\tau_{1,\epsilon}$ and $\omega\tau_{2,\epsilon}$, with $\tau_{1,\epsilon}$ and $\tau_{2,\epsilon}$ being the longest and second longest relaxation times (determined for I-49 and I-I 24-24, respectively).

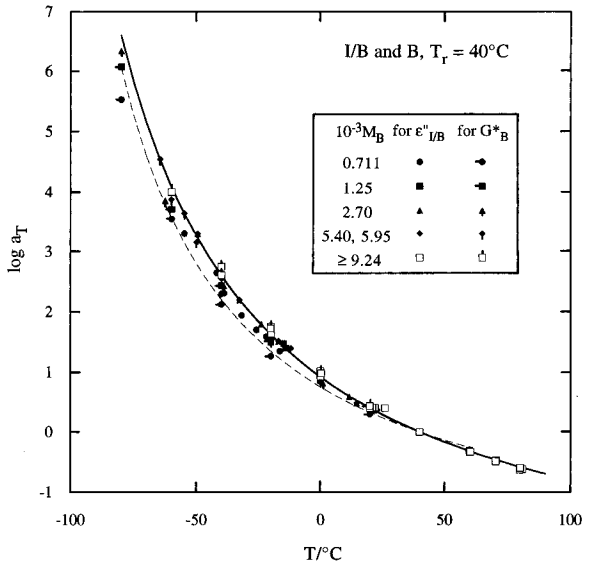

Figure 4. Temperature dependence of shift factors a_T for ϵ'' of dilute PI chains in B matrices (symbols without pips) and for G^* of pure B matrices (symbols with pips). The solid and dashed curves indicate the data obtained by Colby et al.[22] for high-M_B (≥20K) polybutadiene and low-M_B (=1.13K) oligobutadiene, respectively.

for viscoelastic moduli G^* of the pure matrices (symbols with pips). The solid and dashed curves indicate a_T obtained by Colby et al.[22] for high-M_B (≥20K) polybutadiene and low-M_B (=1.13K) oligobutadiene, both reduced at 40 °C by use of their WLF parameters. For

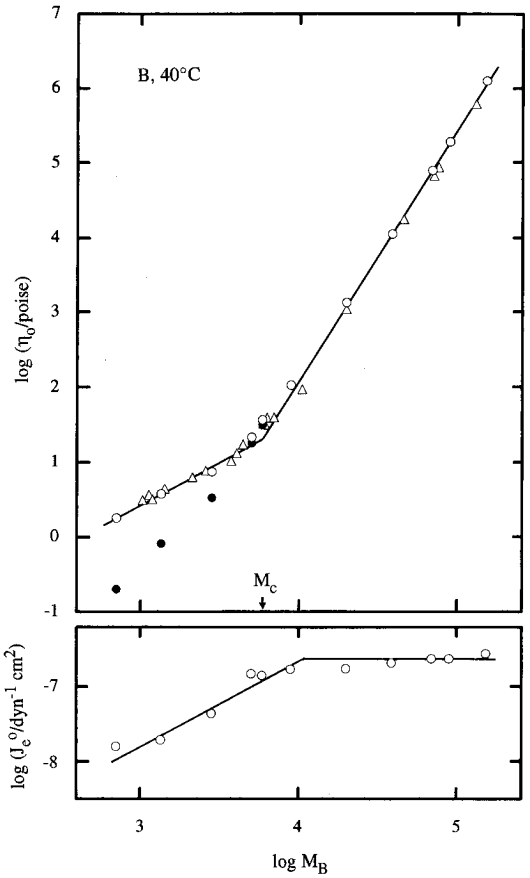

Figure 5. M_B dependence of zero-shear viscosity η_0 and steady-state recoverable compliance J_e^0 for pure B matrices at 40 °C after the correction of segmental friction ζ for M_B < 9.24K (unfilled circles). The data without this correction are indicated with the filled circles. Triangles indicate the η_0 data of Colby et al.[22] reduced to our iso-ζ state.

respective I/B blends, we note good agreements of a_T for ϵ'' and G^* (i.e., for dilute PI and matrix B). The temperature dependence of a_T reflects that of the segmental friction, ζ.[21,22] Thus, the results of Figure 4 indicate that the temperature dependence of ζ is the same for the dilute PI chains and matrices and that ζ for the PI chains is determined by the segmental motion of surrounding matrix chains.[10]

In Figure 4, we also note differences in the temperature dependence of a_T for the PI chains in long ($M_B \geq$ 9.24K) and short (M_B < 9.24K) matrices. These differences are also seen for the data of Colby et al. (solid and dashed curves). The difference is due to the well-known increase in the fractional free volume f with decreasing M_B:[21,22] The shift of the ϵ'' curves toward the high-ω side seen for small M_B < 9.24K (Figure 1) is mostly due to this increase in f and corresponding decrease in ζ for the PI chains.

As done by Colby et al.,[22] standard WLF analysis was carried out for the a_T data of Figure 4, and the WLF parameters C_1 and C_2 were evaluated from plots of $(T_r - T)/(\log a_T)$ against $(T - T_r)$, with T_r being the reference temperature (=40 °C). Then, the ζ-correction factors,[21,22] $\zeta^\infty/\zeta = \exp[2.303(C_1^\infty - C_1)]$, were evaluated for the PI chains in the short matrices of M_B < 9.24K. Here, ζ^∞ and C_1^∞ designate the ζ and C_1 values for the dilute PI chains in long matrices of $M_B \geq$ 9.24K. These ζ^∞/ζ factors agreed with the ζ-correction factors determined for the B matrices and also with those reported by Colby et al.[22]

Figure 5 shows the M_B dependence of η_0 and J_e° for the pure B matrices at 40 °C. For the short matrices

(M_B < 9.24K), the data after the above ζ-correction are shown with the unfilled circles. For those matrices, η_0 without the correction (filled circles) is considerably smaller than the corrected η_0. At the iso-ζ state, our η_0 data (unfilled circles) coincide with the data of Colby et al.[22] (triangles) and exhibit the well-known behavior, $\eta_0 \propto M_B^{3.5}$ (for $M_B > M_c \cong 6$K) and $\eta_0 \propto M_B$ (for $M_B < M_c$). The compliance also exhibits the well-known behavior, $J_e^\circ \propto M_B^1$ (for $M_B < M_c' \cong 13$K) and $J_e^\circ \propto M_B^0$ (for $M_B > M_c'$). The product, $J_e^\circ\eta_0$, gives an average relaxation time that is close to the longest viscoelastic relaxation time, $\tau_{1,G}$.[21] In the following sections small differences between $J_e^\circ\eta_0$ and $\tau_{1,G}$ are neglected, and $J_e^\circ\eta_0$ is used as $\tau_{1,G}$ and compared with dielectric relaxation times of the PI chains. This introduces negligibly small uncertainties in the comparison.

III-2. Dielectric Relaxation Time of Dilute PI Chains. Among the eigenmodes of the local correlation function (cf. eq 3), only odd modes are dielectrically observed for I-49 and I-6 without dipole inversion while only even modes are observed for I-I 24-24 with symmetrical inversion. Thus, the ϵ'' peaks seen in Figure 1 correspond to the slowest odd (first) eigenmode for I-49 and I-6 and to the slowest even (second) eigenmode for I-I 24-24. τ_1 and τ_2 of those modes were evaluated as the reciprocal of the corresponding peak frequencies. (In our previous paper,[10] the relaxation time for the second eigenmode, referred to as τ_2 in this paper, was denoted with the symbol "τ_1" in a sense that τ_2 corresponds to the slowest *dielectric* mode observed for PI chains with symmetrical dipole inversion. In this paper, we have numbered the relaxation time according to the eigenmode index p defined in eq 3.)

Part a of Figure 6 shows the M_B dependence of $\tau_{1,\epsilon}$ (large circles) and $\tau_{2,\epsilon}$ (large squares) for the dilute PI chains examined in Figure 1. (The second subscript, ϵ, explicitly indicates that $\tau_{1,\epsilon}$ and $\tau_{2,\epsilon}$ are the dielectrically determined relaxation times for the PI chains.) $\tau_{1,\epsilon}$ data are shown also for previously examined dilute PI chains (c_I = 6%) with M_I = 13.4K and 23.8K (c_I/c^* = 0.61 and 0.81, respectively).[10] The small circles connected with the thick dashed line indicate the viscoelastic relaxation times of the B matrices, $\tau_{1,G}$ (=$J_e^\circ\eta_0$). All those relaxation times are compared at the iso-ζ state explained for Figures 4 and 5. Part b of Figure 6 shows the M_B dependence of the $\tau_{2,\epsilon}/\tau_{1,\epsilon}$ ratio for the I-I 24-24 chain at that state. As done in our previous work,[14,15] $\tau_{1,\epsilon}$ of this chain was evaluated from $\tau_{1,\epsilon}$ of I-49 after a minor correction for a small M_I difference (cf. Table 1). In both parts a and b, the thin dash−dot and dotted curves represent model predictions discussed in a later section.

As seen in part a of Figure 6, $\tau_{1,\epsilon}$ and $\tau_{2,\epsilon}$ of the dilute I-49 and I-I 24-24 chains at the iso-ζ state are hardly dependent on M_B for M_B < 2.7K. However, those relaxation times increase rather rapidly with further increase in M_B above 5−6K. This M_B value for the onset of rapid increase in τ's is close to the characteristic molecular weight M_c for entanglement of the B matrices (cf. Figure 5). Finally, $\tau_{1,\epsilon}$ of I-49 appears to level off and become independent of M_B for M_B > 89K. This leveling-off behavior is more clearly seen for the shorter PI chains of M_I = 23.8K and 13.4K. Similar behavior was previously found also for $\tau_{2,\epsilon}$.[10] These results indicate that the dilute PI chains of $M_I \geq$ 13.4K are entangled with B matrices of $M_B \geq M_c$: The rapid increase of $\tau_{1,\epsilon}$ and $\tau_{2,\epsilon}$ followed by the gradual leveling-off is due to the increase in the entanglement lifetime (decrease of the constraint release contribution) with increasing matrix $\tau_{1,G}$, as concluded in our previous work.[10,11]

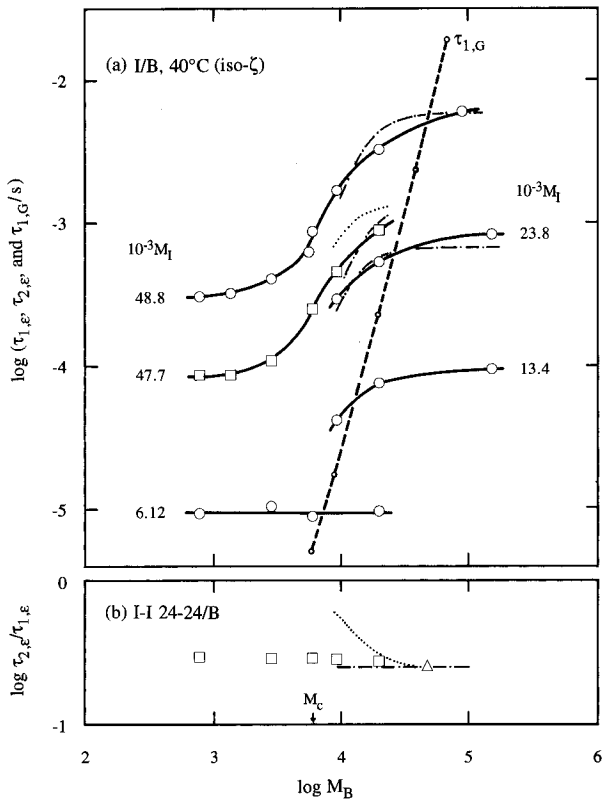

Figure 6. M_B dependence of (a) $\tau_{1,\epsilon}$ and $\tau_{2,\epsilon}$ (large circles and squares) for dilute PI chains in B matrices and (b) $\tau_{2,\epsilon}/\tau_{1,\epsilon}$ ratio for I-I 24-24. Numbers indicate $10^{-3}M_I$. The ζ correction was carried out for the data in matrices of M_B < 9.24 K. The triangle in part b indicates the $\tau_{2,\epsilon}/\tau_{1,\epsilon}$ ratio (=1/3.9) for bulk I-I 24-24. In part a, small circles connected with the thick dashed line indicate the viscoelastic relaxation times $\tau_{1,G}$ (=$J_e^0\eta_0$) for pure B matrices at the iso-ζ state. The thin dash−dot and dotted curves indicate the predictions of the CDCR and CICR models. For details of these models, see text.

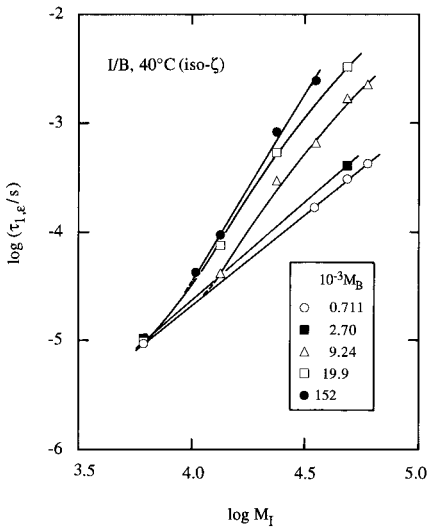

Figure 7. M_I dependence of $\tau_{1,\epsilon}$ for dilute PI chains in B matrices. The ζ correction was carried out for the data in the B-0.7 and B-3 matrices.

In part a of Figure 6, we also note that $\tau_{1,\epsilon}$ of I-6 at the iso-ζ state is quite insensitive to M_B up to M_B = 19.9K ($\cong 3M_c$). Thus, this short PI chain is hardly entangled with the matrices (of any length).

Figure 7 shows the M_I dependence of $\tau_{1,\epsilon}$ for dilute PI chains in the B matrices of various M_B. As done in Figure 6, the data are compared at the iso-ζ state. Figure 7 clearly indicates that the M_I dependence changes with both M_B and M_I: For PI chains entangled

with *much longer* B matrices, $\tau_{1,\epsilon}$ increases rapidly with increasing M_I (filled circles). However, with decrease in M_B (still in the entangled regime), the M_I dependence of $\tau_{1,\epsilon}$ becomes weaker (cf. unfilled squares and triangles). As found previously,[10,11] this change is due to the increase of the constraint release contribution to relaxation of the dilute PI chains. Finally, with further decrease in M_B below M_c, $\tau_{1,\epsilon}$ exhibits a weak M_I dependence in the entire range of M_I. In particular, the M_I dependence in the shortest B-0.7 matrix (unfilled circles) is close to that in low-M solvents (Isopar-G[12] and heptane[13]). The M_I dependence in that matrix is reasonably well described by bead−spring models considering both hydrodynamic and excluded volume interactions.[17]

At this point, we would like to add a few comments on the very recent work by Adachi et al.[6b] They examined the dielectric behavior of I/B blends that are very similar to the blends studied in our previous[10] and present work. They claimed that *at the iso-ζ state* the log $\tau_{1,\epsilon}$ *vs* log M_I plots for dilute PI in various B matrices are represented by straight lines of M_B-dependent slopes and those lines are converged in a point at $M_I = 1.9$K (cf. Figure 5 of ref 6b). However, no such behavior is seen for our data (Figure 7). This difference appears to be almost exclusively due to *insufficient* correction of ζ carried out by Adachi et al.[6b] They did not make the ζ-correction for matrices of $M_B \geq 5.1$K. For shorter matrices, they evaluated the ζ^∞/ζ factor from rather arbitrary superposition of the log a_T *vs* T curves for long and short matrices.[23] Their analysis gave only small ζ^∞/ζ factors: $\log(\zeta^\infty/\zeta) = 0.20$ for $M_B = 2.5$K at 0 °C.[6b] On the other hand, the standard WLF analysis[21,22] for our data (Figure 4) and the data of Colby et al. (Table X in ref 22) give significantly large ζ^∞/ζ factors for $M_B < 9$K that lead to the well-known behavior, $\eta_0 \propto M_B$ for $M_B < M_c$ at the iso-ζ state (Figure 5). Specifically, the WLF analysis for those data gave $\log(\zeta^\infty/\zeta) = 0.55$ for $M_B = 2.5$K at 0 °C, considerably larger than the correction made in ref 6b. This fact strongly suggests the necessity of reexamining the conclusion of Adachi et al.:[6b] Their conclusion for the M_I dependence of $\tau_{1,\epsilon}$ (as well as for the equivalence of the PI and B chains) would be changed if the ζ-correction is properly carried out.

IV. Discussion

IV-1. Relaxation Time of Dilute PI Chains. As seen in Figures 6 and 7, the M_B and M_I dependence of $\tau_{1,\epsilon}$ and $\tau_{2,\epsilon}$ is not the same for the dilute probe PI chains in the nonentangled and entangled states. Thus, we have to separately discuss the dependence for the respective cases.

***τ* for Nonentangled PI.** Figure 6 has indicated that $\tau_{1,\epsilon}$ and $\tau_{2,\epsilon}$ of the long PI chains ($M_I \cong 48$K) at the iso-ζ state are only weakly dependent on M_B in the nonentangling matrices ($M_B < M_c$). In such matrices, the M_I dependence of $\tau_{1,\epsilon}$ becomes gradually weaker with decreasing M_B (cf. filled squares and unfilled circles in Figure 7). In particular, in the shortest B-0.7 matrix, the behavior of the dilute PI chains is essentially the same as the behavior in the usual low-M solvents[17] (Isopar-G[12] and heptane[13]) and thus governed by both hydrodynamic and excluded volume interactions. This result indicates that the free-draining Rouse behavior of the dilute PI chains, if it exists, can be observed only in a rather narrow range of M_B around or slightly below M_c. However, in that range, the dielectric mode distribution of the short I-6 chain is broader than that predicted from the Rouse model (cf. the ϵ'' curve for I-6 in the B-6 matrix with $M_B \cong M_c$; Figure 2). Similar disagreement has been found for the observed and predicted mode distribution for nonentangled bulk PI.[15] Further studies are desired for this problem.

***τ* for Entangled PI.** The M_B dependence of $\tau_{1,\epsilon}$ and $\tau_{2,\epsilon}$ found for $M_B > M_c$ (Figures 6 and 7) indicates that the matrix motion affects the global relaxation of the long, dilute PI chains ($M_I \cong 48$K). As extensively discussed in our previous work,[10,11,14,15,24] this matrix effect is attributed to the constraint release (CR) mechanism[18−20] within the context of generalized tube models.

If the local CR relaxation rate at the nth segment of the dilute PI chains is independent of the chain conformation and the segment coordinates n, competition of CR and reptation mechanisms is described by a configuration-independent CR (CICR) model.[10,11,20,25] As explained previously,[10,11] this model leads to a *factorized* local correlation function that is represented as a product of two independent relaxation functions,

$$C(n,t;m) = \left[\sum_{q=\text{odd}} \frac{8}{q^2\pi^2} \exp[-q^2 t/\tau_{CR}]\right] \times \left[\frac{2}{N}\sum_p \sin\frac{p\pi n}{N} \sin\frac{p\pi m}{N} \exp[-p^2 t/\tau_{rep}]\right] \quad (5)$$

Here, N is the number of segments per PI chain, and $\tau_{CR} = t^\circ_{CR} M_B^3 M_I^2$ and $\tau_{rep} = t^\circ_{rep} M_I^3$ are the CR and reptation times for the PI chain, respectively. In our previous study,[10] the proportionality constants for dilute PI chains in B matrices at 40 °C, t°_{CR} (=8.94×10^{-25} s) and t°_{rep} (=5.03×10^{-17} s), were evaluated from independent dielectric and viscoelastic measurements. From eq 5, the longest relaxation time $\tau_{1,\epsilon}$ and the $\tau_{2,\epsilon}/\tau_{1,\epsilon}$ ratio are predicted as

$$\tau_{1,\epsilon} = [\tau_{CR}^{-1} + \tau_{rep}^{-1}]^{-1}, \quad \tau_{2,\epsilon}/\tau_{1,\epsilon} = [\tau_{CR}^{-1} + \tau_{rep}^{-1}]/[\tau_{CR}^{-1} + 4\tau_{rep}^{-1}] \quad \text{(CICR)} \quad (6)$$

On the other hand, competition of CR and reptation mechanisms is described by a configuration-dependent CR (CDCR) model if the CR relaxation proceeds in a Rouse fashion and the local CR rate is dependent on the chain conformation and segment coordinates.[10,11,20] This model involves the parameters being identical to those for the CICR model. However, differing from the CICR model, the CDCR model gives a *nonfactorized* local correlation function,[10,11]

$$C(n,t;m) = \frac{2}{N}\sum_p \sin\frac{p\pi n}{N} \sin\frac{p\pi m}{N} \times \exp[-p^2 t(\tau_{CR}^{-1} + \tau_{rep}^{-1})] \quad (7)$$

For this case, we find

$$\tau_{1,\epsilon} = [\tau_{CR}^{-1} + \tau_{rep}^{-1}]^{-1}, \quad \tau_{2,\epsilon}/\tau_{1,\epsilon} = 1/4 \text{ irrespective of } M_I \text{ and } M_B \quad \text{(CDCR)} \quad (8)$$

As seen from eqs 6 and 8, the two models predict the same $\tau_{1,\epsilon}$ but different $\tau_{2,\epsilon}$ (or $\tau_{2,\epsilon}/\tau_{1,\epsilon}$ ratio). It should also be noted that the CICR model predicts that the dielectric mode distribution changes with τ_{CR} and τ_{rep} (i.e., with M_I and M_B) while the CDCR model predicts the M_I- and M_B-independent mode distribution.[10,11,20] As explained previously,[10,11] this feature of the CDCR

model results from the coincidence of the reptation and Rouse eigenfunctions for $C(n,t;m)$.

We used the $t°_{CR}$ and $t°_{rep}$ parameters to calculate $\tau_{1,\epsilon}$ and $\tau_{2,\epsilon}$ for the CICR and CDCR models. The results are shown in Figure 6 with the thin dotted (CICR) and dash−dot (CDCR) curves. (Obviously, these models are applicable only in the entangled regime, $M_B > M_c$). The two models reasonably describe the $\tau_{1,\epsilon}$ data (large circles in Figure 6a). However, for $\tau_{2,\epsilon}$ (squares in Figure 6a) and $\tau_{2,\epsilon}/\tau_{1,\epsilon}$ ratio (Figure 6b), the CDCR model describes the data better than the CICR model. Concerning the difference between the two models, we note in Figure 2 that the ϵ'' curve of I-49 exhibits an almost M_B-independent shape for $M_B \geq 9.24$K ($> M_c$). This result is in harmony with the CDCR prediction, but qualitatively different from the CICR prediction: For I-49, the ϵ'' curve calculated from the CICR model actually became sharper with increasing M_B from 9.24K to 89K. (Similar changes in the calculated curve have been shown in Figure 7 of ref 10b.) All these results indicate that the actual CR process has a configuration-dependent nature (as considered in the CDCR model) and its relaxation function does not have a factorized form (eq 5), confirming the conclusion of the previous work.[10,11,24]

However, we would also like to emphasize that even the CDCR model does not perfectly describe the behavior of dilute probe (PI) chains in entangling matrices. We have already specified limitations of this model for dielectric as well as viscoelastic relaxation processes.[10,11,24] An essential point revealed in our recent work[14,15] is the non-Rouse nature of the actual CR processes (and nonreptative nature of actual relaxation in high-M matrices) that are most clearly noted for a nonsinusoidal functional form of the eigenfunctions for $C(n,t;m)$ (cf. eq 3). Details of the actual, non-Rouse CR processes have been discussed elsewhere.[14,15]

IV-2. Equivalence of Probe and Matrix Chains. A blend of dilute probe chains in a *chemically identical* matrix is obviously reduced to a monodisperse homopolymer system if the probe and matrix have the same molecular weight. On the other hand, for the homogeneous blends of chemically different (probe PI and matrix B) chains examined in this paper, the probe and matrix molecular weights are not the straightforward quantities specifying a hypothetical monodisperse state for the probe. Instead, this state is realized when the probe and matrix have the same *relaxation time*.

For *monodisperse* PI chains, Adachi et al.[5] have shown that the viscoelastic relaxation time τ_G is close to the dielectric relaxation time τ_ϵ in the entangled regime and that $\tau_G \cong \tau_\epsilon/2$ in the nonentangled regime. Thus, for respective PI chains examined in this study, the molecular weight M_B* of an *equivalent* B matrix realizing the hypothetical monodisperse state can be determined from the conditions for the matrix relaxation time $\tau_{1,G}$,

$$\tau_{1,G} = \tau_{1,\epsilon} \quad \text{(in the entangled regime)} \quad (9a)$$

and

$$\tau_{1,G} = \tau_{1,\epsilon}/2 \quad \text{(in the nonentangled regime)} \quad (9b)$$

M_B* specified by eq 9a was determined as the intersects between the solid curves ($\tau_{1,\epsilon}$) and the dashed line ($\tau_{1,G}$) shown in Figure 6a. M_B* specified by eq 9b was similarly determined.

Figure 8 shows plots of M_B* against M_I. Unfilled and filled circles indicate M_B* specified by eqs 9a and 9b, respectively. The relationship between $\tau_{1,G}$ and $\tau_{1,\epsilon}$ for

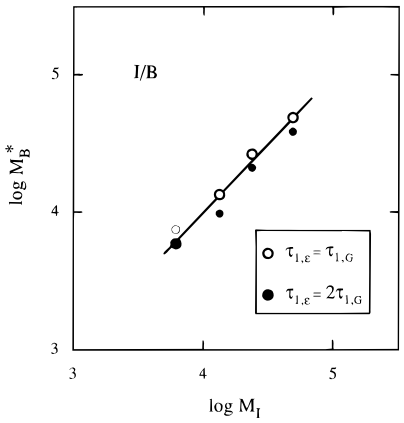

Figure 8. Plots of equivalent matrix molecular weight M_B* against molecular weight of dilute PI chains in B matrices. Unfilled and filled circles indicate M_B* determined from eqs 9a and 9b, respectively. Large circles indicate M_B* specified according to a relationship between $\tau_{1,\epsilon}$ and $\tau_{1,G}$ for monodisperse bulk PI. The solid line indicates a relationship, $M_B* = M_I$.

the monodisperse PI systems[5] suggests that eqs 9a and 9b are to be used for entangled and nonentangled PI chains ($M_I \geq 13.4$ K and $M_I = 6.12$K in Figure 6), respectively. M_B* specified according to this criterion are indicated with the large circles in Figure 8. As seen there, those M_B* data obey a relationship, $M_B* = M_I$ (solid line). We also note that the unfilled and filled circles are closely located and thus the choice of eq 9a or 9b introduces only small uncertainty in the evaluation of M_B*.[26] From these results, we can conclude that dilute PI chains in a B matrix of identical M behave as if they are in the monodisperse bulk state. At the same time, we have to emphasize that this conclusion is obtained for the dilute PI chains (with $c_I \leq c$*) and not necessarily valid for nondilute PI chains (with c_I being considerably larger than c*).

IV-3. Broadening of the Dielectric Mode Distribution. Figure 2 has indicated that the dielectric mode distribution of the dilute PI chains is broadened with increasing matrix molecular weight. As explained below, this change is not due to changes in entanglement effects, the excluded volume interaction, and the hydrodynamic interaction.

We have demonstrated that entangled and nonentangled bulk PI chains have the same mode distribution, and thus entanglement is not responsible for the broadening of the distribution.[10,15] This conclusion is further supported by the results of this study: As seen in Figure 6a, the short I-6 chain has an M_B-independent $\tau_{1,\epsilon}$ and is not entangled with the B matrices examined. Nevertheless, I-6 still exhibits broadening of the mode distribution with increasing M_B (Figure 2).

As explained earlier, the excluded volume interaction is not significant for the short I-6 chain even in the shortest B-0.7 matrix. Thus, the broadening observed for this chain rules out the possibility that the changes in this interaction cause the broadening. This conclusion is further supported by the fact[16] that the mode distribution is the same for dilute, long PI chains in marginal and good solvents (heptane and cyclohexane).

We also note that bead−spring models are reasonably valid in dilute solutions[12,13,17] but incorporation of changes in the hydrodynamic interaction in the models does not explain the observed broadening of the mode distribution.[17] This fact suggests that the changes in this interaction are not responsible for the mode broadening.

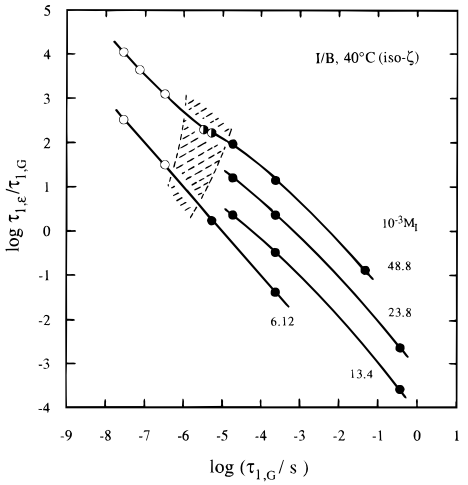

Figure 9. Plots of ratio of relaxation times, $\tau_{1,\epsilon}/\tau_{1,G}$, against $\tau_{1,G}$. The plots are indicated with the filled circles when the PI chains exhibit a broad mode distribution identical to that for bulk PI, with the unfilled circles when the chains have a sharp mode distribution similar to that in dilute solutions, and with the half-filled circles when the mode distribution is between these two extremes. The ζ correction was carried out for the data in matrices of M_B < 9.24K.

As a remaining possibility, we may consider some sort of coupling of the motion of the dilute probe PI chains with the surrounding B matrices. For the simplest case of viscoelastic coupling, the probe chain regards the matrix chains just as a viscous medium and exhibits sharp mode distribution *when the probe/matrix relaxation time ratio ($\tau_{1,\epsilon}/\tau_{1,G}$) is increased above a certain critical value.* For this case, the $\tau_{1,\epsilon}/\tau_{1,G}$ ratio in a crossover zone for the mode broadening should be essentially constant irrespective of $\tau_{1,G}$ and $\tau_{1,\epsilon}$. From this point of view, the nature of coupling is examined in Figure 9, where the $\tau_{1,\epsilon}/\tau_{1,G}$ ratio is plotted against the matrix $\tau_{1,G}$. The sense of the symbols represents the width of the dielectric mode distribution of the PI chains: The plots are indicated with the *filled* circles when the PI chains exhibit a broad mode distribution identical to that for bulk PI, with the *unfilled* circles when the chains have a sharp mode distribution similar to that in dilute solutions, and with the *half-filled* circles when the mode distribution is between these two extremes.

In Figure 9, we first note that the conditions specifying the hypothetical monodisperse state, $\tau_{1,\epsilon}/\tau_{1,G} = 1$ or 2 (cf. eq 9 and Figure 8), are satisfied in the zone of a broad mode distribution (filled circles). This result is in harmony with the broad distribution actually observed for monodisperse bulk PI. More importantly, the $\tau_{1,\epsilon}/\tau_{1,G}$ ratio is not constant but rather strongly dependent on $\tau_{1,G}$ in the hatched, crossover zone for the mode broadening. This result indicates that the coupling of the probe and matrix motion is not of the simple viscoelastic nature.

As explained earlier for eqs 1−4, the mode distribution is determined by the relaxation time span ($\tau_{p,\epsilon}/\tau_{1,\epsilon}$ ratio) and the dielectric intensity (g_p) distribution. Concerning this fact, it should be noted that the observed broadening is associated with only minor changes in the $\tau_{2,\epsilon}/\tau_{1,\epsilon}$ ratio (from 1/3.4 to 1/3.9; cf. Figure 6b). Thus, as found previously,[17] the broadening with increasing M_B should be essentially due to changes in the g_p distribution that result from changes in the eigenfunctions f_p (eq 3) from sinusoidal to nonsinusoidal functions: f_p becomes nonsinusoidal when some mechanism (not considered in Rouse, reptation, and other conventional models) enhances the relaxation at chain ends as compared to the chain center.[14,15,17]

When the motion of the probe and matrix is coupled (not in the simple viscoelastic sense), the probe end motion would be transmitted to the probe center through action of the matrix, and *vice versa*. For this case, the probe end and center should mutually constrain their motion, but the constraint should be smaller for the ends having neighboring segments only in one direction along the chain contour. Thus, the coupling with the matrix seems to less confine, or enhance *in a relative sense*, the relaxation at the chain ends than at the center. This argument suggests that the coupling is certainly a candidate for enhancing the relaxation at chain ends, thereby affecting f_p and the mode distribution. However, any coupling mechanism (such as the previously discussed length variable local jump[15]) can lead to the observed mode broadening if it enhances the relaxation at chain ends. In other words, it is still too early to judge whether the mechanism is the same or not in the entire range of the probe and matrix molecular weights. Examination of the coupling mechanism(s) deserves further attention.

V. Concluding Remarks

We have studied the dielectric behavior of dilute PI chains in B matrices of various M_B. The PI relaxation time $\tau_{1,\epsilon}$ was found to increase with increasing M_B (in the constraint release regime). More importantly, an increase in M_B broadened the dielectric mode distribution of the PI chains. This broadening is not due to changes in the entanglement effects, the excluded volume interaction, and the hydrodynamic interaction. Instead, coupling of the motion of the PI and matrix chains would be the cause of the mode broadening. This coupling mechanism cannot be of a simple viscoelastic nature, as evidenced from the fact that the $\tau_{1,\epsilon}/\tau_{1,G}$ ratio is not constant in the crossover regime for the mode broadening. Further studies are desired for details of the coupling mechanism(s).

Acknowledgment. We thank Dr. A. Kajiwara and Prof. M. Kamachi for their help with oligo-GPC measurements. We acknowledge with thanks the financial support for this study from the Ministry of Education, Japan, under Grant No. 06651054.

References and Notes

(1) Stockmayer, W. H. *Pure Appl. Chem.* **1967**, *15*, 539.
(2) (a) Baur, M. E.; Stockmayer, W. H. *J. Chem. Phys.* **1965**, *43*, 4319. (b) Stockmayer, W. H.; Burke, J. J. *Macromolecules* **1969**, *2*, 647.
(3) Imanishi, Y.; Adachi, K.; Kotaka, T. *J. Chem. Phys.* **1988**, *89*, 7585; see the references therein for the earlier work on polydisperse PI chains.
(4) Yoshida, H.; Adachi, K.; Watanabe, H.; Kotaka, T. *Polym. J. (Jpn.)* **1989**, *21*, 863.
(5) Adachi, K.; Yoshida, H.; Fukui, F.; Kotaka, T. *Macromolecules* **1990**, *23*, 3138.
(6) (a) Adachi, K.; Itoh, S.; Nishi, I.; Kotaka, T. *Macromolecules* **1990**, *23*, 2554. (b) Adachi, K.; Wada, T.; Kawamoto, T.; Kotaka, T. *Macromolecules* **1995**, *28*, 3588.
(7) Yoshida, H.; Watanabe, H.; Adachi, K.; Kotaka, T. *Macromolecules* **1991**, *24*, 2981.
(8) Adachi, K.; Kotaka, T. *Prog. Polym. Sci.* **1993**, *18*, 585; see also the references therein.
(9) Boese, D.; Kremer, F.; Fetters, L. J. *Macromolecules* **1990**, *23*, 829; *ibid.* **1990**, *23*, 1826.
(10) (a) Watanabe, H.; Yamazaki, M.; Yoshida, H.; Adachi, K.; Kotaka, T. *Macromolecules* **1991**, *24*, 5365. (b) Watanabe, H.; Yamazaki, M.; Yoshida, H.; Kotaka, T. *Macromolecules* **1991**, *24*, 5372.
(11) Watanabe, H.; Kotaka, T. *CHEMTRACTS Macromol. Chem.* **1991**, *2*, 139; see also the references therein.

(12) Patel, S. S.; Takahashi, K. M. *Macromolecules* **1992**, *25*, 4382.
(13) Urakawa, O.; Adachi, K.; Kotaka, T. *Macromolecules* **1993**, *26*, 2042.
(14) Watanabe, H.; Urakawa, O.; Kotaka, T. *Macromolecules* **1993**, *26*, 5073.
(15) Watanabe, H.; Urakawa, O.; Kotaka, T. *Macromolecules* **1994**, *27*, 3525.
(16) Urakawa, O. Ph.D Thesis, Osaka University, 1994.
(17) Watanabe, H.; Yamada, H.; Urakawa, O. *Macromolecules* **1995**, *28*, 6443.
(18) Klein, J. *Macromolecules* **1978**, *11*, 852.
(19) Graessley, W. W. *Adv. Polym. Sci.* **1982**, *47*, 67.
(20) Watanabe, H.; Tirrell, M. *Macromolecules* **1989**, *22*, 927.
(21) See, for example: Ferry, J. D. *Viscoelastic Properties of Polymers*, 3rd ed.; Wiley: New York, 1980.
(22) Colby, R. H.; Fetters, L. J.; Graessley, W. W. *Macromolecules* **1987**, *20*, 2226.
(23) Assuming the universal WLF shift on the T_g basis,[21] Adachi et al.[6b] estimated a difference of T_g for high-M_B and low-M_B matrices from rather arbitrary superposition of the log a_T *vs* T curves for those matrices. They reported the difference to be only $\Delta T_g = 6$ K for high-M_B (=5.1−202K) and low-M_B (=2.5K) matrices. This ΔT_g is too small for those matrices, leading to the insufficient ζ-correction made in ref 6b.
(24) Watanabe, H.; Yamazaki, M.; Yoshida, H.; Kotaka, T. *Macromolecules* **1991**, *24*, 5573.
(25) In ref 20, the CICR model was referred to as the extended Graessley model because the CICR model gives a relaxation function Φ being identical to the factorized function deduced from the Graessley model,[19] $\Phi(t) = \Phi_{rep}(t)\,\Phi_{CR}(t)$.
(26) As noted in Figure 6a, eqs 9a and 9b are satisfied when the $\tau_{1,\epsilon}$ *vs* M_B plots are leveling off. In addition, $\tau_{1,G}$ exhibits a strong M_B dependence, $\tau_{1,G} \propto M_B^{3.5}$. For these reasons, the M_B* values determined from eqs 9a and 9b are different only by a samll factor $\cong 2^{1/3.5} \cong 1.2$. For the same reasons, the M_B* values hardly change even if small differences between the longest viscoelastic relaxation time and $J_e^0\eta_0$ (used as $\tau_{1,G}$) are considered in the evaluation of M_B*.

MA9507608